

SOLVENT INDUCED CAGE RECOMBINATION IN CLUSTER IONS: EXPERIMENTAL AND THEORETICAL INVESTIGATIONS

R. PARSON, N. DELANEY, A. SANOV AND W. C. LINEBERGER

*JILA and Department of Chemistry and Biochemistry, University of Colorado
Boulder CO 80309-0440 USA*

E-mail: wcl@jila.colorado.edu, rparson@jila.colorado.edu

Photofragmentation of size-selected $I_2^-(CO_2)_n$ cluster ions and the subsequent cage recombination of the photodissociated I_2^- chromophore are observed to occur with high efficiency and on a ps time scale, for even partially solvated ions. This result is observed for dissociation on either ground state ($\Gamma + I$) or spin-orbit excited ($\Gamma + I^*$) state surfaces. With intimate interplay between theory and experiment, we deduce the importance of solvent induced perturbation of the electronic structure of the chromophore. The dissociation dynamics are well described by a simulation that incorporates non-adiabatic curve crossings and solvent perturbation of the electronic structure within a classical molecular dynamics simulation. When the full dynamics are reduced to a solute and a solvent coordinate, a Marcus-like picture of solvent asymmetry-induced electron transfer emerges as an accurate description of the cage recombination process.

1 Introduction

The dramatic effects of solvation on the outcomes and rates of chemical reactions have motivated many experimental and theoretical studies of reactions in solutions and clusters. A topic of particular interest is the solvent-induced recombination, or “caging” of photofragments [13,30]. While many groups have studied caging in high-pressure gases, matrices, and liquids, the microscopic details of the reaction in these environments are often obscured by the multitude of local solvent configurations and inherent inability of resolving separate product channels. Our groups have emphasized a joint experimental and theoretical investigation of the dynamics of dihalogen anion recombination in size-selected clusters. By placing the greatest emphasis on those components of cluster dynamics that experiment and theory each do best, it has proven possible to obtain a detailed understanding of the caging dynamics in much larger systems than **either** theory or experiment alone could convincingly address. We now describe such a study of the effect of solvent asymmetry in promoting recombination in photodissociated $I_2^-(CO_2)_n$ cluster ions.

2 Methods

2.1 Experimental Methods

The measurements reported here concern the photodissociation of I_2^- in size-selected $I_2^-(CO_2)_n$ ions, with $n < 20$. The excess electron in the cluster remains largely localized on the I_2^- chromophore, and thus the I_2^- potential energy diagram [8,33] shown in Fig. 1

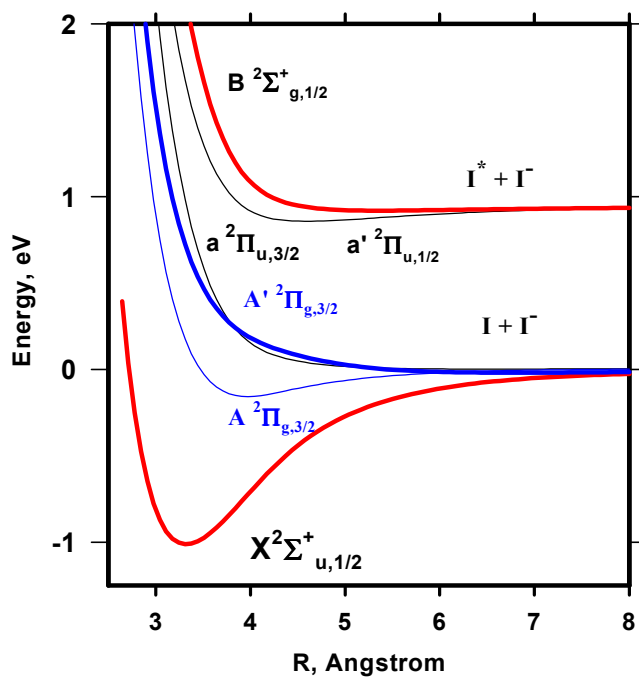


Figure 1. Potential Energy Curves for low-lying states of I_2^- .

provides a starting point for understanding the cluster photophysics. We are concerned with photoexcitation to the A' state, which dissociates to I^- and ground state I, and to the B state, which in the isolated molecule dissociates to I^- and I^* , spin-orbit excited iodine. The experimental apparatus described below allows us to identify caging of the

photodissociated I_2^- and in the absence of caging to distinguish between photofragments exiting on the $\Gamma + I^*$ and the $\Gamma + I$ surfaces.

A complete description of the ion beam apparatus has been given elsewhere [22]. Basically, cold cluster anions are formed in an electron impact ionized supersonic jet expansion and subsequently size-selected in a time-of-flight mass spectrometer. The $I_2^-(CO_2)_n$ cluster ions are formed [14] by attachment of slow secondary electrons to neutral clusters in an electron-impact ionized supersonic jet, with subsequent nucleation around the negatively charged core. A pulsed laser beam is directed onto a specific ion mass, e.g., $I_2^-(CO_2)_{12}$, and the ionic chromophore is photodissociated. A second, reflectron mass spectrometer [1,17] identifies the ionic photoproducts that arise in the first few microseconds following photodissociation.

Two types of experiments are carried out with this apparatus. The first identifies the products of photoexcitation and infers the caging fraction [26,31]; the electronic state (I or I^*) of an iodine atom that escapes the solvent cage is determined from product distributions. The second class of experiment employs ultrafast pump and probe lasers to examine the time dependence of the cage recombination process [16,31]. In both cases, determination of the number of solvent molecules lost from the ionic photoproducts provides the key to identify the states involved.

Photodissociation of $I_2^-(CO_2)_n$ clusters through excitation to the $A'^2\Pi_g$ state leads (in general) to two types of ionic fragments: (1) “caged” $I_2^-(CO_2)_k$ products and (2) “uncaged” $\Gamma(CO_2)_m$ products [26,27]. In both channels, the excess excitation energy is removed from the cluster by evaporation of CO_2 solvent molecules. If the solvent binding energy to the cluster is known (as in this case), then the average number of solvent molecules lost by the cluster provides direct information about the exit (I or I^*) channel in the uncaged case.

Excitation of the $B^2\Sigma_{g,1/2}^+ \leftarrow X^2\Sigma_{u,1/2}^+$ transition (see Fig. 1) at 395 nm in bare I_2^- leads exclusively to dissociation on the spin-orbit excited $\Gamma + I^*(^2P_{1/2})$ asymptote, 0.93 eV above the ground state. However, in the presence of the solvent, dissociation on **both** $\Gamma + I^*$ and $\Gamma + I$ spin-orbit asymptotes is observed for some cluster sizes. The two uncaged channels are unequivocally distinguished by the difference (four) in the **average** number of solvent molecules lost [23].

2.2 Theoretical methods

Solvated molecules or ions present a serious challenge to molecular dynamics simulation, since the interaction between the charge distribution on the solute ion and the surrounding molecules gives rise to strong solvent perturbations of the solute electronic structure. The reaction dynamics must therefore be regarded as taking place on

multidimensional potential energy surfaces that cannot be represented in terms of pairwise interactions at any level of approximation. In 1996 two groups independently met this challenge by devising effective Hamiltonian models of the electronic structure of the interacting solute-solvent system. Coker and co-workers [2,19] based their model on a generalized diatomics-in-molecules Hamiltonian, while Parson's group [5,9,20] relied on a distributed multipole analysis of the one-electron density matrix obtained from an *ab initio* calculation of the solute electronic structure. In the basis defined by the electronic states of the isolated solute, the diagonal elements of the distributed multipole operators describe the charge distribution in the various solute states, while the off-diagonal terms describe transition charge distributions that account for the polarization of the solute wave function by the solvent. In both simulation algorithms, a Hamiltonian matrix whose elements are functions of the solvent degrees of freedom is constructed and diagonalized at each time step of a molecular dynamics trajectory, providing the energies, forces, and nonadiabatic transition probabilities required to propagate the trajectory to the next step [9]. These simulations have successfully reproduced the basic trends in the experimental product distributions, absorption recovery [6], and femtosecond photoelectron spectra [10], and have clarified the interpretation of these trends [28].

3 Observations

A remarkable property of these systems, first seen in the experiments more than a decade ago, is the very high caging efficiency. In the near-IR photodissociation of $I_2^-(CO_2)_n$, for example, the probability of recombination reaches 100% for a single complete solvent shell around the ion, and clusters possessing less than half a solvent shell induce recombination as much as 50% of the time [31]. This behavior is in marked contrast to neutral I_2 , for which caging never reaches 100% even in the bulk liquid. The absorption recovery experiments demonstrate that the overall time scale for dissociation, recombination, and vibrational relaxation is usually about 10-20 ps [25,31], similar to that for I_2^- in liquid solution [15,32] but an order of magnitude larger than that for neutral I_2 . Recombination can take place either directly on the ground state, or indirectly through the weakly bound *A* state, which is subsequently quenched to the ground state. These observations have been confirmed by femtosecond photoelectron spectroscopy [3,11,12], which provides a complementary view of the dynamics, and reproduced by the simulations.

The results of near-UV photodissociation experiments are even more surprising. In this case the initially excited *B* state of I_2^- correlates to spin-orbit excited Iodine, or I^* .

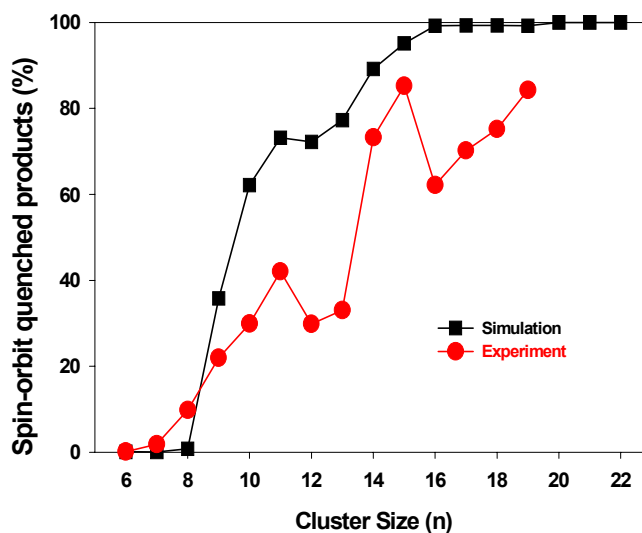


Figure 2. I* quenching percentage as a function of the number of CO₂ solvents (n) in the I₂⁻(CO₂)_n cluster.

The very large (0.94 eV) energy gap between I and I* might lead one to expect that electronic relaxation to states correlated with ground state I should be extremely improbable. Nevertheless, both experiment [29] and simulation [7] find that this becomes a dominant channel in clusters having more than eight or nine CO₂ molecules (Fig. 2). The time required for the electronic relaxation process is about 5 ps – a million-fold enhancement over gas-phase collisional quenching of I* by CO₂. This stark contrast demonstrates that interpretations based solely upon the potential curves of the isolated molecule can lead to qualitatively false conclusions.

4 Interpretation

These unusual results lead one to look for mechanisms that would cause solvated molecular ions to behave in a radically different fashion from their neutral analogs. One such mechanism is intramolecular charge flow: as the solute dissociates, the electronic charge, which was initially delocalized over the molecule, becomes localized on a single I atom, and this changing charge distribution couples the solute electronic structure to

the dynamics of the surrounding solvent. This interplay has some surprising consequences, of which the most dramatic is “anomalous charge flow”: following photoexcitation, the charge moves towards the *less* solvated atom as the molecule dissociates [8,21]. The long-range coulomb force between the departing ion and the residual cluster provides a rationale for the unusually high caging efficiency. This counterintuitive behavior of the solute charge can be understood in terms of simple molecular-orbital pictures or polarizability theory, but the most fruitful interpretation makes use of an analogy with the theory of electron transfer reactions in solution. This analogy builds on the work of Hynes, Barbara, Benjamin, and Gertner, who showed that the recombination of I_2^- on the electronic ground state could be viewed as a special type of electron transfer process [4]. By extending their approach so as to incorporate electronic excited states, we are able provide a comprehensive physical picture of the dynamics that follow photoexcitation.

In the theory of electron transfer reactions [18,24], one begins with “donor” and “acceptor” sites immersed in a polarizable medium. The charge hops from donor to acceptor at a rate that depends on the local energies of the two sites and on the strength of the electronic coupling between them. At the beginning of the reaction the solvent stabilizes the charge on the donor, and transfer of the electron is accompanied by reorganization of the solvent into a configuration that favors the acceptor. The reaction coordinate for this process thus lies within the solvent, and can be conveniently expressed as the electrostatic potential difference $\Delta\Phi$ between the donor and the acceptor sites. The magnitude of $\Delta\Phi$ is small when the solvent molecules are nearly equally shared between the two sites (a “symmetric” cluster) and large when one site is preferentially solvated (an “asymmetric” cluster). At large internuclear distances it is convenient to start with a diabatic representation, in which the electronic coupling is neglected, so that the electronic charge distribution stays fixed as the solvent molecules move. If we sketch the energies of the diabatic states as a function of $\Delta\Phi$, we obtain a pair of “Marcus parabolas” corresponding to an electron localized on either site. When we restore the electronic coupling, the diabatic curves are transformed into adiabatic curves having an avoided crossing at $\Delta\Phi = 0$.

In order to adapt this two-state picture for solvated I_2^- , which has an electron configuration corresponding to one hole in a closed valence shell, we need to expand the state space to include the three p-orbitals on each atom. In the Hund’s Case (c) representation (appropriate for I atoms), one gets three pairs of diabatic Marcus parabolas (Fig. 3). Two of these pairs, corresponding to the two possible alignments of ground state I with respect to the internuclear axis, are nearly degenerate, while the third is displaced upwards by the spin-orbit splitting in the I atom. Again, the intersections

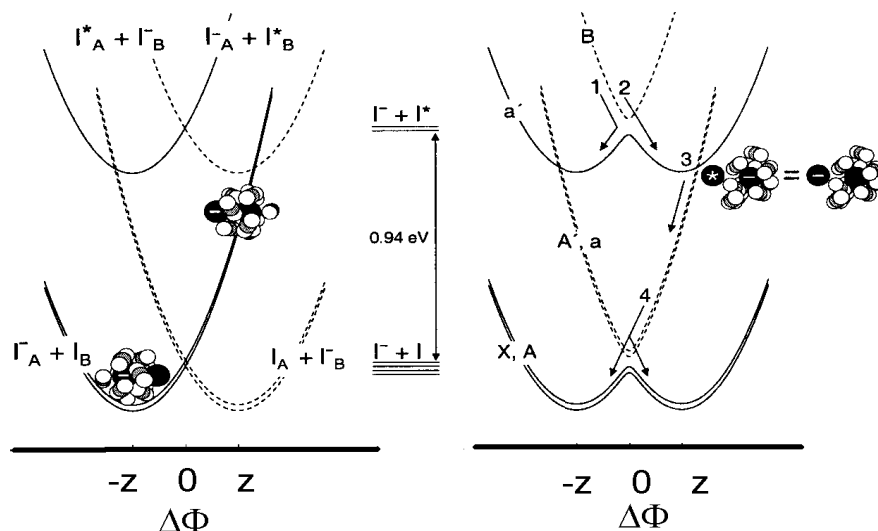


Figure 3. Effect of solvation on dihalide electronic structure at intermediate to long bond lengths, in the limit of large spin-orbit coupling.

between diabatic curves are replaced by avoided crossings in the adiabatic representation. This view of the solvent effects, utilizing condensed phase concepts, provides a framework to interpret the cluster experimental data.

We can use the four lower curves in Fig. 3 to understand the near-IR experiments, in which the spin-orbit excited states do not participate directly. Immediately after excitation, the atoms are close together and the electronic coupling is large, so the adiabatic representation is appropriate. Consider the behavior of the electronic charge distribution as the system moves along the adiabatic curves. On the lower two adiabats, corresponding to the X and A states of the molecule, charge and solvent move in phase with each other. As the solvent coordinate changes sign, the electronic wave function smoothly transforms from one localized on I_A to one localized on I_B , in accord with the traditional picture of adiabatic electron transfer. On the *upper* two (A' , a) curves, however, the charge and solvent must move in opposite directions, since the left-hand limb of the upper adiabat arises from the diabatic curve whose minimum is on the right, and vice versa. This is precisely the phenomenon of “anomalous charge flow,” or negative electronic polarizability. As the atoms move farther apart, the adiabatic curves come very close together so nonadiabatic transitions are likely. A simple diabatic passage through the crossing region, in which the system hops from the upper to the

lower adiabat as the solvent coordinate passes through zero, corresponds to a “solvent transfer” event, in which the charge distribution stays fixed while the solvent moves towards the charge. In a nonadiabatic charge transfer event, in contrast, the charge switches from one atom to the other as the solvent coordinate approaches zero, and the solvent then reverses direction. Both mechanisms have been seen in the simulations [5,19], and both lead to a charge distribution that is stabilized by the solvent on the lower state. Thus anomalous charge flow, which dominates during the first 500 fs after dissociation, reverts to normal charge flow on longer time scales. The strong attractive forces between Γ^- and the residual cluster in the initially excited “anomalous” state prevent direct dissociation on this state; instead dissociation only occurs after an electronic transition to one of the lower states. Both the high overall caging efficiency and the time scales for recombination on the ground and excited states are explained in this fashion.

To understand the results of the UV experiments, we need all six of the states in Fig. 3. Now photoexcitation brings the system high up on the wall of the B state. Again, nonadiabatic solvent-transfer and charge-transfer transitions out of this anomalous state can take place as the solvent coordinate passes through zero. Once on the “normal” a' state, however, the system may go on to encounter the intersections with the A' and a states that occur at large values of the solvent coordinate. In the diabatic representation, these crossings correspond to points where the difference between the solvation energy of the Γ^- ion and the I neutral is approximately equal to the atomic spin orbit energy of I^* . A passage through the crossing then corresponds to the **resonant** transfer of an electron from a solvated I_B^- to an I_A^* atom on the outside of the cluster, resulting in I_A^- on the outside and I_B in its electronic ground state on the inside. Solvent-driven electron transfer thus provides a mechanism for efficient electronic quenching of the spin orbit excited states. This mechanism only operates in the larger clusters, those having eight or more CO_2 molecules, because in the smaller clusters there are not enough solvent molecules available to bring the solvent coordinate $\Delta\Phi$ into the neighborhood of 1 eV.

5 Conclusion

The intimate interplay between theory and experiment described here has proven to be an exhilarating experience, enabling far greater progress in understanding many body behavior in complex systems than was possible with either alone. While those of us in the cluster research community have long considered clusters as a bridge for understanding the evolution from the gas phase to the condensed phase, the work reported here treats a cluster as a unique state of matter. The cluster does not merely

mimic the condensed phase with size selection added, but it introduces an asymmetric environment that is more extreme than can readily be encountered in bulk matter. This inherent asymmetry in partially solvated ions affords access to solvent electric fields that emphasize solvation effects in ways that enable enhanced understanding of them. By casting the interpretation of the cluster simulations in the language of condensed phases and Marcus theory, it has been possible to clarify microscopic understanding of the original condensed phase theory. Finally, it has been crucial to have reliable experimental data involving the same chromophore as a bare ion, in size-selected clusters, and in a variety of solvents. Without this experimental foundation, the simulations of large systems with multiple surface crossings would not be compelling.

6 Acknowledgements

We thank our colleagues and collaborators, especially Jim Faeder, Paul Maslen, John Papanikolas, and Todd Sanford, for their many important and continuing contributions to the work summarized here. This research has been supported by the National Science Foundation and the Air Force Office of Scientific Research. A. Sanov is now located at the Department of Chemistry, University of Arizona, Phoenix, AZ 85721.

References

1. Alexander M. L., Ph.D. Thesis, University of Colorado, 1987.
2. Batista V. S. and Coker D. F., *J. Chem. Phys.* **106**, 7102 (1997).
3. Batista V. S., Zanni M. T., Greenblatt B. J., Neumark D. M. and Miller W. H., *J. Chem. Phys.* **110**, 3736 (1999).
4. Benjamin I., Barbara P. F., Gertner B. J. and Hynes J. T., *J. Phys. Chem.* **99**, 7557 (1995).
5. Delaney N., Faeder J., Maslen P. E. and Parson R., *J. Phys. Chem. A* **101**, 8147 (1997).
6. Delaney N., Faeder J. and Parson R., *J. Chem. Phys.* **111**, 452 (1999).
7. Delaney N., Faeder J. and Parson R., *J. Chem. Phys.* **111**, 651 (1999).
8. Faeder J., Delaney N., Maslen P. E. and Parson R., *Chem. Phys. Lett.* **270**, 196 (1997).
9. Faeder J., Delaney N., Maslen P. E. and Parson R., *Chem. Phys.* **239**, 525 (1998).
10. Faeder J. and Parson R., *J. Chem. Phys.* **108**, 3909 (1998).
11. Greenblatt B. J., Zanni M. T. and Neumark D. M., *J. Chem. Phys.* **111**, 10566 (1999).

12. Greenblatt B. J., Zanni M. T. and Neumark D. M., *J. Chem. Phys.* **112**, 601 (2000).
13. Harris A. L., Brown J. K. and Harris C. B., *Ann. Rev. Phys. Chem.* **39**, 341 (1988).
14. Johnson M. A. and Lineberger W. C., in *Techniques for the study of ion molecule reactions*, edited by J. M. Farrar and J. W. Saunders (Wiley, New York, 1988), pp. 591.
15. Kliner D. A. V., Alfano J. C. and Barbara P. F., *J. Chem. Phys.* **98**, 5375 (1993).
16. Lineberger W. C., Nadal M. E., Nandi S., Wenthold P. G., Kim J. B., Andersen L. H., Ozaki Y. and Boo D. W., in *Femtochemistry and femtobiology: Ultrafast reaction dynamics at atomic-scale resolution. Nobel symposium 101*, Vol. 101 (Imperial College Press, London, 1998), pp. 423.
17. Mamyrin B. A., Karataev V. I., Shmikk D. V. and Zagulin V. A., *Sov. Phys.-JEPT* **37**, 45 (1973).
18. Marcus R. A., *Ann. Rev. Phys. Chem.* **15**, 155 (1964).
19. Margulis C. J. and Coker D. F., *J. Chem. Phys.* **110**, 5677 (1999).
20. Maslen P. E., Faeder J. and Parson R., *Mol. Phys.* **94**, 693 (1998).
21. Maslen P. E., Papanikolas J. M., Faeder J., Parson R. and O'Neil S. V., *J. Chem. Phys.* **101**, 5731 (1994).
22. Nadal M. E., Kleiber P. D. and Lineberger W. C., *J. Chem. Phys.* **105**, 504 (1996).
23. Nandi S., Sanov A., Delaney N., Faeder J., Parson R. and Lineberger W. C., *J. Phys. Chem.* **102**, 8827 (1998).
24. Newton M. D. and Sutin N., *Ann. Rev. Phys. Chem.* **35**, 437 (1984).
25. Papanikolas J. M., Campagnola P. J., Vorsa V., Nadal M. E., Buchenau H. K., Parson R. and Lineberger W. C., in *The chemical dynamics and kinetics of small radicals*, Vol. 6, edited by K. Liu and A. Wagner (World Scientific Publishing Co., Singapore, 1995), pp. 616.
26. Papanikolas J. M., Gord J. R., Levinger N. E., Ray D., Vorsa V. and Lineberger W. C., *J. Phys. Chem.* **95**, 8028 (1991).
27. Papanikolas J. M., Vorsa V., Nadal M. E., Campagnola P. J., Buchenau H. K. and Lineberger W. C., *J. Chem. Phys.* **99**, 8733 (1993).
28. Parson R., Faeder J. and Delaney N., *J. Phys. Chem. A*, in press (2000).
29. Sanov A., Sanford T., Nandi S. and Lineberger W. C., *J. Chem. Phys.* **111**, 664 (1999).
30. Troe J., *Ann. Rev. Phys. Chem.* **29**, 223 (1978).
31. Vorsa V., Nandi S., Campagnola P. J., Larsson M. and Lineberger W. C., *J. Chem. Phys.* **106**, 1402 (1997).
32. Walhout P. K., Alfano J. C., Thakur K. A. M. and Barbara P. F., *J. Phys. Chem.* **99**, 7568 (1995).
33. Zanni M. T., Taylor T. R., Greenblatt B. J., Soep B. and Neumark D. M., *J. Chem. Phys.* **107**, 7613 (1997).